Datta, A., Devismes, S., Horn, F., and Larmore, L. (2011). Self-stabilizing k-out-of-l exclusion in tree networks. Int. J. Found. Comput. Sci., 22(3):657-677.

Datta, A., Hadid, R., and Villain, V. (2003a). A new self-stabilizing k-out-of- l exclusion algorithm on rings. In Self-Stabilizing Systems, ser. Lecture Notes in Computer Science, S.-T. Huang and T. Herman, Eds., 2704:113-128.

Datta, A., Hadid, R., and Villain, V. (2003b). A self-stabilizing token-based k-out-of-l exclusion algorithm. Concurrency and Computation: Practice and Experience, 15:1069 -1091.

Dijkstra, E. (1974). Self stabilizing systems in spite of distributed control. Communications of the Association of the Computing Machinery, 17:11:643{644.

Dolev, D., Gafni, E., and Shavit, N. (1988). Toward a non-atomic era: l -exclusion as test case. Proceeding of the 20th Annual ACM Symposium on Theory of Computing, Chicago, pages 78-92.

Dolev, S., Israeli, A., and Moran, S. (1997). Uniform dynamic self-stabilizing leader election. IEEE Transactions on Parallel and Distributed Systems, 8:4:420-440.

Fisher, M., Lynch, N., Burns, J., and Borondin, A. (1979). Resource allocation with immunity to limited process failure. Proceedings of the 20th IEEE Annual Symposium on Foundations of Computer Science, pages 234-254.

Fisher, M., Lynch, N., Burns, J., and Borondin, A. (1989). A distributed fifo allocation of identical resources using small shared space. ACM Transactions Programming Languages Systems, 11:90-144.

Flatebo, M., Datta, A., and Schoone, A. (1994). Self-stabilizing multi-token rings. Distributed Computing, Vol. 8, 8:133{142.

Gartner, F. (2003). A survey of self-stabilizing spanning-tree construction algorithms. School of Computer and Communication Sciences, Technical Report IC/2003/38.

Gouda, M. and Haddix, F. (1996). The stabilizing token ring in three bits. Journal of Parallel and Distributed Computing, 35:43-48.

Gradinariu, M. and Tixeuil, S. (2001). Tight space self-stabilizing uniform l-mutual exclusion. Distributed Computing, Vol. 7, pages 83-90. 32

Hadid, R. (2000). Space and time efficient self-stabilizing l -exclusion in tree networks. Proceedings of the 14th IEEE International Parallel and Distributed Processing Symposium, pages 529-534.

Hadid, R. (2002). Space and time efficient self-stabilizing l -exclusion in tree networks. Journal of Parallel and Distributed Computing, 62(5):843-864.

Hadid, R. and Villain, V. (2001). A new efficient tool for the design of self-stabilizing l -exclusion algorithms: the controller. In Proceedings of the 5th IEEE International Work-shop, WSS, pages 137-151.

Masum, S., Akbar, M., Ali, A., and Rahman, M. (2010). A consensus-based l -exclusion algorithm for mobile ad hoc networks. Ad Hoc Networks Journal, 8:30-45.

Peterson, G. (1990). Observation on l -exclusion. Proceedings of the 28th Annual Allerton Conference on Communication, Control and computing, Monticello, pages 568-577.

Villain, V. (1999). A key tool for optimality in the state model. In DIMACS'99, The 2nd Workshop on Distributed Data and Structures, Carleton University Press, pages 133-148.

Submitted : *06/03/2013*
Revised : *15/07/2013*
Accepted : *03/12/2013*

Journal of Engg. Research **Vol. 2 - (1) March 2014** pp. 121-132

تحليل قياسات شعاع الأيون لمعامل هول للتشتت في شريحة السيليكون المزروع بالانتيموني للنوع العادي والمشدود

***طلال الزنكي، *** نيك بينيت، **رسل جوليم، **كريسجينز، ****بول بيلي، ****تيم نواكس، و**برين سيلي**

*قسم الهندسة الإلكترونية - كلية الدراسات التكنولوجية- الهيئة العامة للتعليم التطبيقي والتدريب -الكويت
**كلية الهندسة والفيزياء -جامعة سيري - المملكة المتحدة
*** كلية الهندسة الالكترونية - جامعة مدينة دبلن - أيرلندا
****داسبري ميس مختبر - داسبري - المملكة المتحدة

خلاصة

لقد تم إستخدام طريقتى النثر الخلفى-رذرفورد (RBS) ونثر أيون الطاقة المتوسطة (MEIS) لتحديد شعرية موقع الأنتيمونى (Sb) المزروع في السيليكون العادي (Si) والسليكون المشدود (sSi) عند مستوى طاقة أيون تتراوح من 2keV إلى 40keV. وقد تم إستخدام معامل هول لقياس النسب المئوية للنشاط الكهربائى بعد تصلب العينات تحت درجات حرارة تتراوح من 600 الى 1100 سليزية وفي أوقات مختلفة. وتم عمل مقارنة بين شعرية موقع التركيز ونسب النشاط الكهربائى للتأكد من أن معامل هول للتشتت يساوى وحدة واحدة. وبينت النتائج أن التفعيل الكهربائى للأنتيمونى المزروع بلغ 90٪ عند مستوى 40keV بينما بلغ من 10٪ إلى 80٪ عند مستوى 2keV وذلك حسب جرعة الأيونات المزروعة وحالة التصلب. ويرجع النقصان فى مستوى التفعيل الكهربائى الى عدم فعالية الأنتيمونى المجاور لسطح طبقة السيليكون والأوكسيد الأصلى أو لكون التركيز أكبر من $4.5x10^{20}cm^{-3}$. إن عملية الشد تسهل تواجد الأنتيمونى فى شعرية الموقع والتفعيل الكهربائى لها فى السيليكون نتيجة لأرتفاع جرعة الأيونات المزروعة. وقد تم عمل مقارنة لطريقتى النثر الخلفى ونثر أيون الطاقة المتوسطة مع قاعدة بيانات معامل هول لتبين ان معامل هول للتشتت يساوى وحدة واحدة للأنتيمونى المزروع فى السيليكون العادى والمشدود ضمن حدود الخطأ المختبرى.

Ion Beam Analysis for Hall Scattering Factor Measurements in Antimony Implanted Bulk and Strained Silicon

TALAL ALZANKI*, NICK BENNETT**, RUSSELL GWILLIAM***, CHRIS JEYNES***, PAUL BAILEY****, TIM NOAKES****AND BRIAN SEALY***

**Dept.of Elect. Eng., College of Technical Studies, Public Authority for Applied Education & Training, Kuwait.*

***Dept.of Elect. Eng., Dublin City University, Ireland.*

****Dept.of Elect. Eng., University of Surrey, Surrey, United Kingdam.*

*****Lab. of MEIS,Daresbury, Cheshire, United Kingdam.*

ABSTRACT

Rutherford back-scattering (RBS) and Medium Energy Ion Scattering (MEIS) have been used to determine the lattice site occupancy of antimony (Sb) implanted into silicon (Si) and strained silicon (sSi) for ion energies of 2keV to 40keV. After annealing in the range 600-1100°C for various times, Hall effect measurements were used to provide a measure of the percentage electrical activity. A comparison of the lattice site occupancy with the percentage electrical activity was used to confirm whether the assumption that the Hall scattering factor is equal to unity is valid. Our results demonstrate that for 40keV implants the electrical activation is about 90%. In the case of 2keV implants the electrical activation is lower and in the range 10-80%, depending on the ion fluence and annealing conditions. This reduction in activation for lower energy implants is a result of inactive Sb close to the semiconductor/native-oxide interface, or above concentrations of $4.5x10^{20}cm^{-3}$. Tensile strain facilitates the lattice site occupancy and electrical activation of Sb in Si by raising the doping ceiling. For both 40keV and 2keV implants, we have carried out a comparison of RBS/MEIS and Hall effect data to show that for Sb implants into both bulk Si and strained Si the Hall scattering factor is equal to unity within experimental error.

Keywords: Rutherford backscattering; Medium Energy Ion Scattering; Hall scattering factor; Hall effect; rapid thermal annealing; antimony; bulk silicon; strained silicon.

INTRODUCTION

We have been studying Sb implants into Si for some time to ascertain if such implants might be used to replace arsenic (As) as the main n-type dopant in the production of integrated circuits, particularly those based on CMOS devices. We have published many of our findings (Alzanki *et al.*,2004; Sealy *et al.*,2006; Alzanki *et al.*, 2006; Bennett *et al.*, 2006; Bennett *et al.*, 2008(A); Bennett *et al.*, 2008(B); O'Reilly *et al.*, 2008; Bennett *et al.*, 2008(C); Alzanki *et al.*, 2009; Lai *et al.*, 2009) on implants with ion energies ranging from 2keV up to 40keV and fluences between 10^{14} cm^{-2} and 10^{15} cm^{-2}, typical of implants used in the manufacture of modern CMOS devices. In this paper we will summarise our results of Rutherford back-scattering (RBS) analyses of these materials, and also present Medium Energy Ion Scattering (MEIS) data which demonstrate a much improved sensitivity to depth than RBS does. We will relate the structural data such as lattice site location to electrical data from Hall effect and sheet resistance measurements in order to quantify the magnitude of the Hall scattering factor, a necessary consideration when making Hall measurements. The essential presence of a magnetic field in order to make a Hall measurement can provoke varying degrees of carrier scattering that distort the measured carrier concentration and Hall mobility, requiring a correction factor. The Hall scattering factor (r) affects the sheet carrier density (Ns) and conductivity mobility (μ_C) according to

$$Ns = \frac{r}{e.RHs} \tag{1}$$

$$\mu_C = \frac{RHs}{r.\rho_S} = \frac{\mu_H}{r} \tag{2}$$

where RHs is the sheet Hall coefficient, ρ_S is sheet resistivity, μ_H is Hall mobility and e is the charge of an electron (or a hole) [Hall *et al.*,1925]. While r is mathematically simple to apply, it is however difficult to attain analytically because of the complicated scattering mechanisms involved and differences depending on dopant species (Norton *et al.*, 1973). An added complication becomes apparent when we compare Hall measurements on doped Si substrates with those on doped strained silicon, where the Hall scattering factor might be affected by strain Romano *et al.* (2003).

EXPERIMENTAL METHOD

Implants into bulk (100) p-type silicon wafers and commercially available strained silicon wafers, 17.5nm thick grown on $Si_{0.83}Ge_{0.17}$ relaxed buffer layers,

were carried out at room temperature with a 7° tilt and 22° rotation. Defect-free growth on relaxed buffer layers containing 17% Ge in the SiGe creates a strain of -0.7% in the overlying silicon layer. Strained layers were grown below critical thickness (Matthews *et al.*, 1974) to ensure that the layers did not relax upon thermal treatment. This was confirmed by post-annealing X-ray diffraction measurements (Bennett *et al.*, 2008(C)).The antimony was implanted at 2keV, 5keV and 40keV to fluences in the range $1x10^{14}$ to $1x10^{15}$ cm^{-2}. After implantation the wafers were cut into small pieces and activated using a Process Products Corporation RTP system in the temperature range from 600°C to 1100°C for times between 5 seconds and 3600 seconds in flowing nitrogen gas. However, the majority of samples were annealed for 10s as longer annealing times produced little difference in electrical activity or sheet resistance. Annealing above 800°C allowed the antimony to in-diffuse.

Samples were analysed both before and after annealing using Rutherford backscattering (RBS) and Medium Energy Ion Scattering (MEIS). The RBS and channelling measurements employed a 1.56 MeV $4He^+$ beam with a detector at a scattering angle of 147°. Depth profiles were extracted from non-aligned spectra with the DataFurnace fitting code (Jeynes *et al.*,2003). MEIS was performed at the Daresbury Laboratory using the double alignment mode with the [$\hat{1}\hat{1}\hat{1}$] as the channeling direction, the incident angle was 54.7° [111] and the scattering angle was 70.5°. The analyzing beam was 100keV He^+ ions and the blocking direction was [111] which formed the best compromise between high depth resolution and sufficient mass separation. The former requires maximizing the path lengths of the He^+ ions in the sample so that inelastic energy loss per unit depth inside the silicon is as great as possible, whilst the latter demands maintaining a sufficient energy difference between the Si and O and Si and Sb peaks in the spectra, respectively, such that the overlap between deeper lying Si damage peaks and the O peak or deeper Sb and Si is avoided, as reported previously (Collart *et al.*, 2002). RBS and MEIS in conjunction with channeling have been used to determine the substitutional fraction of the antimony implant after annealing, to measure the retained fluence and to monitor gross diffusion during annealing.Sheet Hall effect measurements were performed on Van der Pauw cloverleaf-shaped samples to determine the active carrier density. Cloverleaf patterns were fabricated using lithographic patterning and mesa etch using a hydrofluoric/nitric acid. Secondary Ion Mass Spectroscopy (SIMS) was used to determine antimony atomic profiles both before and after annealing. The measurements were carried out using a CAMECA IMS 6F with a primary beam energy of 750eV O_2^+ for 5 - 40keV antimony, whilst for the 2keV antimony a 500eV Cs^+ beam was used for the analysis. The lower primary beam energy was chosen to ensure that SIMS gives reliable profile shape and dose in the near-surface regions (Mount *et al.*, 1998). The work of (Nylandsted-Larsen

et al.,1986)has shown that RBS measurements can give an over-estimated substitutional Sb fraction for doping profiles with Sb concentrations in excess of $4.5x10^{20}cm^{-3}$, since above this threshold Sb tends to cluster with vacancies, or form precipitates at elevated temperatures. Sb contained in Sb-vacancy complexes occupies near-substitutional lattice sites and appears as substitutional Sb in channelling experiments. However, the Sb atoms do not contribute electrically. In order to identify the effects of Sb complexes, these experiments were designed with a range of maximum Sb concentrations that were determined by SIMS (Figure 1).

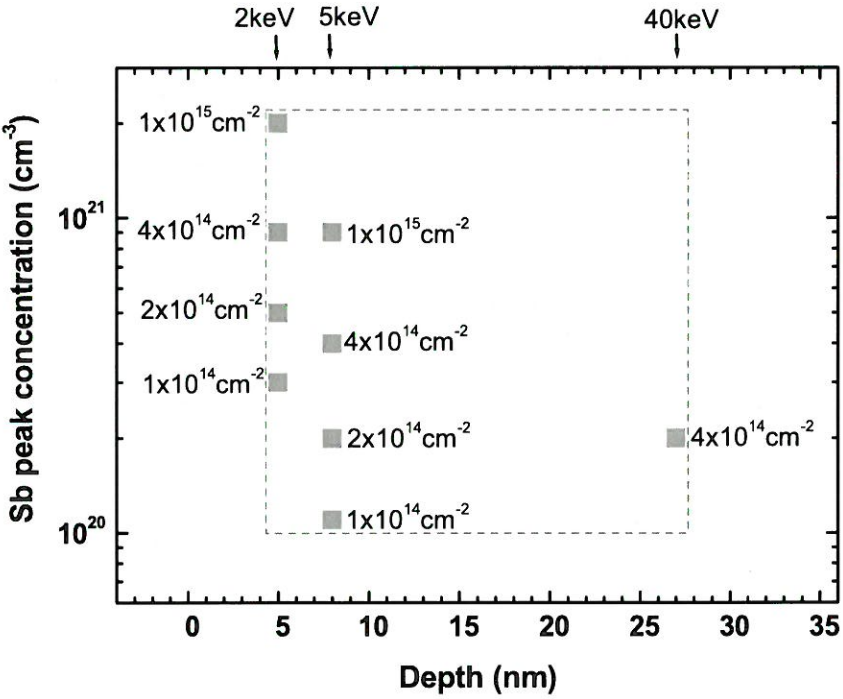

Fig. 1. Sb peak concentration as a function of peak depth for the full range of Sb implants used in this study. Arrows at the top indicate ion energy. Sb fluence is marked next to each point. Data points are extracted from SIMS measurements.

RESULTS

Figure 1 summrises the SIMS data for ion energies of 2 keV, 5 keV and 40 keV. Subsequently we chose samples implanted at 2 keV and 40 keV to perform a detailed study, assuming the results for 5 keV would be somewhere between these two extremes of ion energy.Thus, in this section the results for 40 keV implants are presented first, followed by a more detailed analysis of 2 keV

implants. Table I shows that for 40keVSb implants in bulk Si, the substitutional fraction measured by RBS is higher (nearly 100%) for annealing temperatures at and below 900°C but decreases with increasing annealing temperature. The counting statistics uncertainty of the substitutional fraction is about 2% and there is no significant difference in the substitutional fraction for annealing temperatures below 900°C. A similar trend is seen for the electrical fraction measured using the Hall effect, where the error in the Hall activation is approximately 3%. Consequently the electrical activation and the substitutional fraction are equal within experimental error for annealing temperatures of 1000^0C and below.

The substitutional fraction is higher than the electrical activation after annealing at 1100^0C which suggests that some antimony atoms are on lattice sites but not electrically active. Most probably they are in the form of complexes with neighbouring vacancies (Nylandsted-Larsen *et al.*,1986). The fact that the substitutional fraction and the electrical activity are equal in the case of interest - where we have the highest electrical activation - is in accord with our assumption that the Hall scattering factor is unity, at least for this concentration of antimony atoms implanted into (100) silicon at room temperature.

Table I. Average values over wafer of Electrical activation (Hall) and substitutional fraction (RBS) for 40 keV Sb in silicon as a function of annealing temperature for 30s anneals and for a nominal fluence* of $4x10^{14}cm^{-2}$.

Annealing temperature (C)	Substitutional fraction Sb (%)(±2%)	Electrical activation (%)(±3%)
700	94	90
800	95	88
900	90	88
1000	85	83
1100	72	62

***Note fluence from RBS for as implanted and all annealed samples is 3.9 +/-0.3x10^{14} cm^{-2}.**

Next we turn our attention to the (2keV) implants for which all results are givenin Table II. However we did carry out some preliminary measurements at a fluence of $1x10^{15}$ cm^{-2} before studying the lower flunces in detail. For a nominal fluence of 10^{15} cm^{-2}, the retained fluence for samples annealed at 600-800°C, using both SIMS and RBS, were found to be 8.2 $x10^{14}$ cm^{-2} and $8.1x10^{14}$ cm^{-2} respectively. This result demonstrates that it is important to check the retained fluence in all implants in order to generate an accurate value for the electrical activation. For this high fluence, the sheet carrier concentration showed that only 12% of the retained fluence was electrically activated in bulk Si. Because

RBS becomes insensitive much below a fluence of $1x10^{15}Sbcm^{-2}$, we performed SIMS analysis and found that for fluences of $1x10^{14}cm^{-2}$, $2x10^{14}cm^{-2}$ and $4x10^{14}cm^{-2}$, the retained fluence was again about 80% of the nominal implanted fluence. The dose loss is suspected to result from the proximity of the Sb implant to the Si surface. RBS of 40keV implants at a fluence of $4x10^{14}cm^{-2}$ showed much less evidence of segregation towards the surface and a build up of Sb in interstitial positions following annealing at 1000 °C and 1100 °C for 10s (Alzanki *et al.*, 2004). The active fraction for 2keV implants at ion fluence of $1x10^{14}cm^{-2}$ and $2x10^{14}cm^{-2}$ is around 80% for both MEIS and Hall measurements and for annealing at temperatures of 600, 700 or 800°C for 10s. This is true for implants in both bulk Si and sSi. At the higher annealing temperature of 900°C Sb deactivation occurs corresponing to a lower temperature than was evident for 40keV Sb implants comparing Table I and Table II. This difference is probably related to having a higher peak Sb concentration in the 2keV experiments (see Figure 1). Work by (Takamura *et al.*, 2004) illustrates this concentration-temperature dependent deactivation particularly well, whereby deactivation occurs at lower temperatures when the Sb maximum concentration is increased (Takamura *et al.* 2004).

Table II. Substitutional fraction (MEIS) and Electrical activation (Hall) as a function of annealing temperature, fluence and substrate for 2keV Sb implants annealed for 10s.

Substrate	Fluence (cm^{-2})	Anneal temperature (^0C)	Substitutional fraction Sb (%)(±2%)	Electrical activation (%)(±3%)
Bulk	$1x10^{14}$	600	79	80
Bulk	$1x10^{14}$	700	82	78
Bulk	$1x10^{14}$	800	77	75
Bulk	$1x10^{14}$	900	66	62
Bulk	$2x10^{14}$	700	64	65
Bulk	$4x10^{14}$	As-implanted	8	-
Bulk	$4x10^{14}$	600	36	33
Bulk	$4x10^{14}$	700	67	30
Bulk	$4x10^{14}$	800	70	19
Bulk	$4x10^{14}$	1100	52	-
sSi	$1x10^{14}$	700	77	78
sSi	$2x10^{14}$	700	80	84

Figure 2 shows MEIS (a) random and (b) channeled spectra of 2keV antimony as a function of annealing temperature. In Figure 2(a), for a fluence of

$4x10^{14}$ cm^{-2}, there is some small movement of the antimony towards the surface even at 700°C but no in-diffusion. The behaviour is similar at 800°C and as the temperature is increased the effect becomes more pronounced, which suggests that the antimony segregates towards the surface, perhaps as a result of oxidation or from a 'snow-plough' effect during solid-phase epitaxial regrowth. Comparing aligned spectra (a), with channeled spectra (b), shows that at temperatures of 700°C and above there is a peak in the non-substitutional fraction close to the surface. Thus, antimony moves towards the surface where it probably forms precipitates and becomes electrically inactive. The substitutional fraction shown in Table II is a maximum of about 70% at 700°C and 800°C, although the electrical activation is much lower at these two temperatures. Only at 600°C does the substitutional fraction equate to the electrical activation. For this higher fluence it seems that the MEIS over-estimates the substitutional fraction. It is likely this occurs because the majority of the implanted Sb is contained in concentrations in excess of $4.5x10^{20}cm^{-3}$ in the form of clusters and precipitates. Sb contained in these complexes occupies near-substitutional lattice sites and appears as substitutional Sb in channelling experiments even though it does not contribute electrically (Nylandsted-Larsen *et al.*,1986).

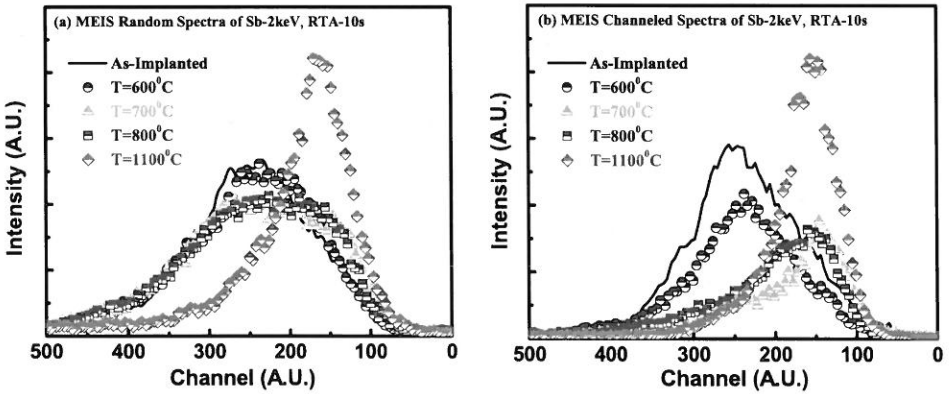

Fig. 2. MEIS (a) random and (b) channeled spectra of 2keV antimony as a function of annealing temperature for bulk si and a fluence of $4x10^{14}cm^{-2}$.

In Figure 3 MEIS data is presented for 2keV, $2x10^{14}cm^{-2}$ Sb implants in Si and sSi, respectively. In these plots approximately 20% of the implanted Sb is located in non-substitutional, electrically inactive sites, near the sample surface. Substitutional and electrical fractions from these spectra are also presented in Table II. In this case the substitutional fraction measured by MEIS is in good agreement with the electrical fraction measured using the Hall effect. For this fluence, the Sb peak is at ~$5x10^{20}cm^{-3}$, i.e. the MEIS result is not significantly

distorted by Sb complexes. The good agreement between MEIS and Hall measurements for both Sb-implanted Si and sSi suggests that the Hall scattering factor is close to unity in both substrates. One point of note is that for this Sb fluence the substitutional and electrical Sb fraction for Si and sSi become less similar. For a fluence of $1x10^{14}cm^{-2}$ the Sb fractions were ~80% in both Si and sSi. For a fluence of $2x10^{14}cm^{-2}$ the electrical and substitutional fraction remains at ~80% in strained Si, but is reduced to ~65% in bulk Si. This supports our previous electrical data suggesting Sb has a higher active solubility in sSi than in Si (Bennett *et al.*, 2008(C)). As well as the near surface inactive Sb in both samples, which accounts for ~20% of the fluence, more Sb is inactive at or around the peak of the profile in the Si sample, suggesting the solubility limit is lower in the bulk Si case. This finding is explained by a strain-compensation argument whereby tensile lattice strain encourages the incorporation of large Sb atoms in the host lattice (Ahn *et al.*, 2009).

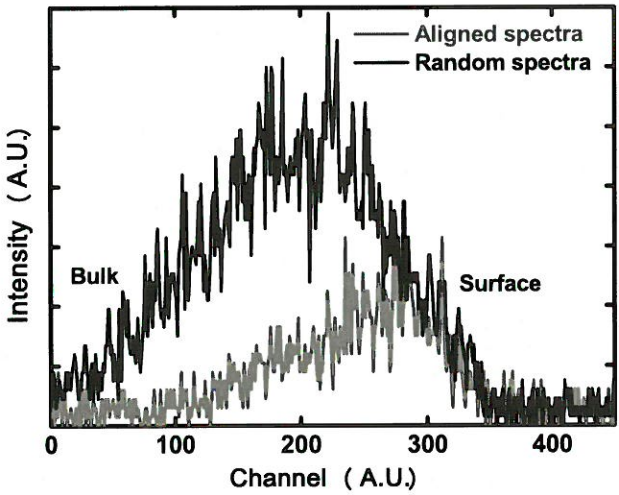

Fig. 3a. Random and aligned MEIS spectra for Sb in (2keV, $2x10^{14}cm^{-2}$) bulk silicon sample, annealed at 700°C for 10s.

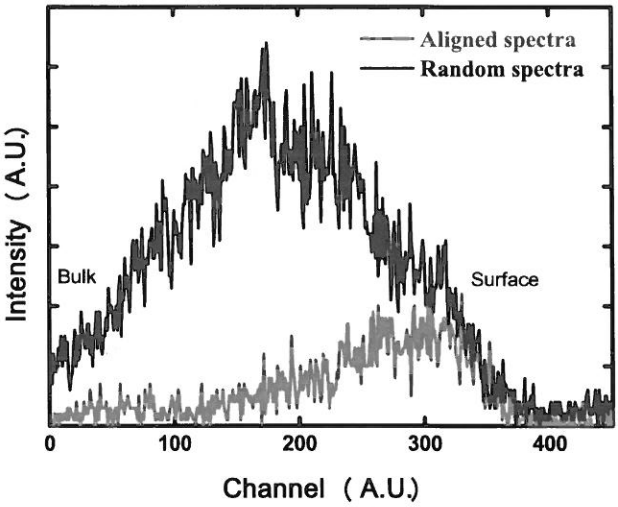

Fig. 3b. Random and aligned MEIS spectra for Sb in (2keV, $2x10^{14}cm^{-2}$) strained silicon sample, annealed at 700°C for 10s.

CONCLUSIONS

Rutherford back-scattering and Medium Energy Ion Scattering have been used to determine the lattice site occupancy of antimony implanted into silicon and strained silicon for ion energies of 2keV and 40keV. After annealing in the range 600-1100^{0}C for various times, Hall effect measurements were used to provide a measure of the percentage electrical activity. A comparison of the lattice site occupancy with the percentage electrical activity was used to confirm the assumption that the Hall scattering factor is equal to unity. Our results demonstrate that for 40keV implants the electrical activation is about 90%. In the case of 2keV implants the electrical activation is lower and in the range 10-80%, depending on the fluence and annealing conditions. This reduction in activation for lower energy implants is a result of inactive Sb close to the semiconductor/native-oxide interface, or above a concentration of $4.5x10^{20}cm^{-3}$. Tensile strain facilitates the lattice site occupancy and electrical activation of Sb in Si by raising the doping upper limit. For doping profiles with peak concentrations in excess of the doping ceiling one should exercise caution when using channeling to look at substitutional Sb. Sb appearing on substitutional sites in channeling experiments might not contribute electrically. For 2keV implants, we have carried out a comparison of MEIS and Hall effect data to show that for Sb implants into both bulk Si and strained Si layers the Hall scattering factor is equal to unity within experimental error.

ACKNOWLEDGEMENTS

The authors thank the Kuwait Government, this work has been supported by the Public Authority of Applied Education and Training (PAAET) of the State of Kuwait (grant TS-09-03)&(grant TS-11-08). We also thank the University of Surrey Ion Beam Centre and the United Kingdom (UK) Engineering and Physical Sciences Research Council (EPSRC) for financial support of this project.

REFERENCES

Ahn, C. Bennett, N.S. Dunham S. T.& Cowern, N.E.B. 2009. Stress effects on impurity solubility in crystalline materials: A general model and density-functional calculations for dopants in silicon. Physical Review **B 79**: 073201-073204.

Alzanki, T. 2004. Antimony implants for ultra-shallow junctions in silicon..PhD Thesis.University of Surrey. United Kingdom (UK).

Alzanki, T.Gwilliam, R. Emerson, N. Smith, A. Webb, R.& Sealy, B. J. 2006. Electrical profiles of 20nm junctions in Sb implanted silicon. Nuclear Instruments and Methods in Physics Research **B242**: 693-695.

Alzanki, T. Gwilliam, R. Emerson, N. & Sealy, B. J. 2009. Low energy antimony implantation in p-type silicon for ultra-shallow junction formation. Kuwait Journal of Science and Engineering. **36 (2B)**:107-115.

Bennett, N.S., Cowern, N. Smith, A.,Gwilliam, R, Sealy, B. J., O'Reilly, L. McNally, P.J. Cooke, G. &Kheyrandish, H. 2006. Highly conductive Sb-doped layers in strained Si. Applied Physics letters **89**: 182122.

Bennett, N.S., Smith, A.J.,Gwilliam, R.M., Webb, R.P., Sealy, B.J., Cowern, N.E.B., O'Reilly,L., & McNally, P.J. 2008(A). Antimony for n-type metal oxide semiconductor ultrashallow junctions in strained Si: a superior dopant to arsenic?. Journal of Vacuum Science and Technology**B26**: 391-395.

Bennett, N.S. Radamson, H. Beer, C. Smith, A. Gwilliam, R, Cowern, N, &Sealy, B.J. 2008(B). Enhanced n-type dopant solubility in tensile-strained Si. Thin Solid Films **517**: 331-333 **Bennett, N.S. 2008(C).** Ultrashallow Junctions for Strain-Engineered NMOS Devices.PhD Thesis.University of Surrey. United Kingdom (UK).

Collart, E. Kirkwood, D.Vandervorst, W.Brijs, B.Van den Berg,J. A.Werner, M.&Noakes, T.C.Q.2002. Characterisation of low Energy Antimony (2-5 keV) Implantation into Silicon. Proceeding of IEEE International. Conference Ion Implant technology: 147-150.

Hall, E. H.1925. Measurement of the Four Magnetic Transverse Effects. Physical Review **26(6):** 820-840.

Jeynes,C.Barradas, N. P. Marriott,, P. K. Boudreault, G. Jenkin, M. Wendler, E.& Webb, R. 2003. Elemental thin film depth profiles by ion beam analysis using simulated annealing - a new tool. Journal of Physics **D**: Applied Physics **36:** R97.

Lai, Y. Bennett, N.S. Ahn, C. Cowern, N.E.B. Cordero, N.&Greer, J. C.2009. Transient activation model for antimony in relaxed and strained silicon. Solid-State Electronics. **53(11):** 1173-1176.

Matthews, J. W. &Blakeslee, A. E J. 1974. Defects in epitaxial multilayers *: I. Misfit dislocations.Journal of Crystal Growth. **27:** 118-125.

Mount, G.R., Smith, S.P., Hitzman, C.J., Chia, V.K.F, Magee, C.W., 1998. Ultra-shallow junction measurements: A Review of SIMS Approaches for Annealed and Processed Wafers. AIP Conf. Proc. **449**: 757-765.

Norton, P. Braggins, T. &Levinstein H. 1973. Impurity and Lattice Scattering Parameters as Determined from Hall and Mobility Analysis in n-Type Silicon. Physical Review **B8**: 5632-5653.

Nylandsted-Larsen, A.Pedersen, F. T. Weyer, G. Galloni, R. Rizzoli, R. &Armigliato, A. 1986. The nature of electrically inactive antimony in silicon. Journal of Applied Physics. **59(6):** 1908-1918.

O'Reilly, L. Bennett, N.S. McNally, P.J. Sealy, B.J., Cowern, N.E.B. Lankinen, A. Tuomi, T. O. 2008. Journal of Materials Science: Materials in Electronics **19**: 305-309.

Romano, L. Napolitani, E. Privitera, V. Scalese, S. Terrasi, A. Mirabella, S.& Grimaldi, M. G. 2003. Carrier concentration and mobility in B doped Si_1Ge_x. Materials Science and Engineering. **B102**: 49-52.

Sealy, B. J. Smith, A. Alzanki, T. Bennett, N.S. Li. L, Jeynes, C. Colombeau. C, Collart. E, Gwilliam, Emerson, N. & Cowern, N. 2006. Shallow junctions in silicon via low thermal budget processing. IWJT International Workshop on Junction Technology: 10-15.

Takamura, Y. Marshall, A. F. Mehta, A. Griffin, P. B. Plummer, J. D.& Patel, J. D. 2004. Diffuse x-ray scattering and transmission electron microscopy study of defects in antimony-implanted silicon. Journal of Applied Physics **95(8):**3968-3977.

Submitted : *10/02/2013*
Revised : *08/09/2013*
Accepted : *30/10/2013*

Journal of Engg. Research **Vol. 2 - (1) March 2014** pp. 133-146

تحليل إحصائي لأداء أكوام إسمنت بورتلاند المحتوي مخلفات سيراميك زجاجية

***أ. تيبيك و **ز. ج. ألتين**

*جامعة يلاوا، كلية الهندسة، قسم الهندسة الصناعية، يلاوا، تركيا
وجامعة أيدن اسطنبول، كلية الآداب والعلوم، قسم الإحصاء، تركيا
**جامعة يلدز التقنية، قسم الهندسة الكيميائية، اسطنبول، تركيا

خلاصة

الهدف من هذه الدراسة هو فحص اعادة استخدام مخلفات صناعات البلاط كبديل لمادة البوزلان الطبيعية (NP) تم فحص الخواص الكيميائية والفيزيائية لخليط ثنائي من إسمنت بورتلاند ومخلفات سيراميك زجاجي. وتم قياس معامل القوة بإضافة كميات من مخلفات السيراميك بنسب وزنية بنسبين هي:

(٪40، 30، 20، 10، 5) ولمدد معالجة هي: 90، 56، 28، 7، 2 يوم.

أظهرت النتائج أن توقيت الإعدادات النهائية لمعجون الإسمنت تم تسريعها عندما استبدلت مادة البوزلان الطبيعية بإضافة المخلفات وظهرت قيم جيدة لقوة الضغط لنسبة مخلفات أقل من 15٪. لوحظ انخفاض في قوة الضغط عند زيادة نسبة المخلفات. النتائج الاحصائية أظهرت أن مخلفات السيراميك الزجاجية بديل رئيسي لمواد الإسمنت التكميلية. استخدام نسبة أقل من 15٪ من مخلفات السيراميك يمكن أن يكون بديلا لمادة البوزلان الطبيعية. وأظهرت النتائج زيادة في قوة الضغط مع زيادة نسبة المخلفات حتى 10٪ مقارنة مع العينات التي استخدمت كمرجع.